Commun.Fac.Sci.Univ.Ank.Series B
Volume 61, Number 1-2, Pages 31-54 (2019)
ISSN 2687-4806
http://communications.science.ankara.edu.tr/index.php?series=B

DFT CALCULATIONS OF BENZOISOXAZOLE DERIVATIVES

EZGİ ÖZEN, MELİKE KALKAN AND PERVİN ÜNAL CİVCİR

ABSTRACT. In this work, we carried out theoretical calculations to determine the structure-activity relationship and the properties of two benzoisoxazole derivatives. For the quantum chemical calculations, the Density Functional Theory (DFT) with B3LYP (Becke three-parameter hybrid correlation functional combined with Lee–Yang–Parr correlation functional) and 6-311+G(d,p) basis set were employed both in the gas phase and in different solvents such as toluene, chloroform, THF, DCM, acetone, DMSO. The CPCM (conductor-like polarizable continuum) solvation model was also used to compute condensed-phase energies in solvent systems. The structural parameters (bond lengths, bond angles, and dihedral angles), energetics (the total energies, the zero-point vibrational energies, the frontier orbital energies (E_{HOMO}, E_{LUMO}), and the bandgap energies) and the spectroscopic characteristics (UV, IR, ^{1}H-NMR, and ^{13}C-NMR) of the target molecules were also determined. The results of the calculations were compared with experimental values for molecule 1, which exists in literature. The calculated geometries (bond length, bond angle and dihedral angle) were in a good agreement with the experimental data. In the case of IR frequencies, the scaled calculated frequencies agreed reasonably well with the experimental results. Moreover, there is a good correlation between experimental and calculated proton signals ($R^2 = 0.9769$) and carbon signals ($R^2 = 0.9972$) of molecule 1.

1. INTRODUCTION

Heterocyclic compounds are very important in chemistry because of their biological activities. These type of compounds are used commonly in medicinal chemistry and they used to build therapeutic agents. Benzoxazole and benzoisoxazole compounds are the significant class of heterocyclic compounds. Benzoisoxazole derivatives bearing various substituents are known to have diverse biological activities in pharmaceutical and agricultural areas [1]. Some derivatives are also used as semiconductors and as corrosion inhibitors in fuels and lubricants [2]. They are also important intermediates in the synthesis of many complex natural products [3]. Among these compounds, 3-substituted-1,2-benzoisoxazole and its derivatives have significant pharmacological and biological activities such as analgesics [4], anticonvulsant [5,6], antipsychotic [7,8], anticancer [9], antimicrobial [10] and also show an affinity for serotonergic and dopaminergic receptors. For example, 1,2-benzoxazole-3-methanesulfonamide, known as zonisamide, is an effective commercially

Received by the editors: August 02, 2019; Accepted: August 23, 2019.
Key word and phrases: Benzoisoxazoles, Density Functional Theory, IR, UV, NMR.

available antiepileptic. Therefore, synthesis of nitrogen, oxygen and sulfur-containing heterocyclic compounds are of interest to researchers.

In this work, theoretical investigations of 3-(chloromethyl)-6,7-dimethylbenzo[d]isoxazole **1** and 3-(bromomethyl)-6,7-dimethyl benzo[d]isoxazole **2** were performed and their structures and IUPAC names are presented in Fig. 1. In 2011, molecule **1** was synthesized by Arava et al. [11]. However, there is not a synthesis of molecule **2** in literature. Literature survey also reveals that to the best of our knowledge, neither structural properties nor spectral properties of the molecules (**1** and **2)** by quantum chemical calculations have been reported so far. In this context, we aimed to illuminate the structure of the target molecules with the help of quantum chemical calculations considering the biological properties mentioned above and to see how the properties of the bromine-linked derivative of the benzoisoxale ring change concerning the chlorine derivative. Also, we wanted to test the accuracy and reliability of the level of theory and the basis set, which we used in the calculations, by comparing the experimental values to the calculated values of molecule **1**. For these purposes, the structural properties (bond lengths, bond angles, and dihedral angles), energetics (the total energies, the zero-point vibrational energies, the frontier orbital energies (E_{HOMO}, E_{LUMO}), and the bandgap energies), and spectroscopic characteristics (UV-VIS, FT-IR, ^{1}H-NMR, and ^{13}C-NMR) of compounds **1** and **2** were calculated and the results of the calculations were compared with experimental ones for molecule **1,** which exists in the literature [11].

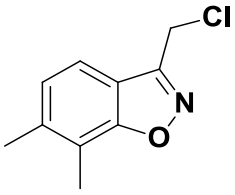

3-(Chloromethyl)-6,7-dimethylbenzo[d]isoxazole **1**

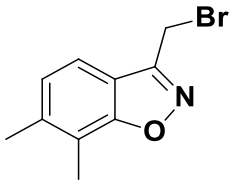

3-(Bromomethyl)-6,7-dimethylbenzo[d]isoxazole **2**

FIGURE 1. Molecular structures and IUPAC names of the studied compounds.

2. Computational Methods

The Density Functional Theory (DFT) [12] calculations presented in this work were carried out by using the Gaussian 09W (Revision D.01) program package [13] and Gauss View 5.0.8 molecular visualization program [14]. Conformation analysis was performed by using B3LYP (Becke three-parameter hybrid functional combined with Lee–Yang–Parr correlation functional) method [15, 16] and the 6-311+G(d,p) basis set [17]. Once the stable conformers

of the target molecules were verified, full geometry optimizations for only the most stable (global minimum on the potential energy surface) conformers were carried using the B3LYP with 6-311+G (d, p) basis set in the gas phase. The B3LYP /6-311+G (d, p) level of theory was selected according to literature examples for this type of molecules [18].

Geometry optimizations were performed with the full analytical Hessian calculated at every geometry step and without any geometrical or symmetry constraints. The vibrational analysis shows that all optimized configurations have no imaginary frequencies and were minima on potential energy surfaces. Harmonic frequencies were used to calculate the zero-point vibrational energies (ZPVE) which was scaled by a factor of 0.967 (B3LYP/6-311+G(d,p)) [18]. This was necessary due to the very complicated structure of the PES, particularly for the larger molecular species. All reported energies are 0 K values including ZPVEs unless otherwise stated. Based on these approaches, the following sections are arranged and our results provide a better understanding of the energetics, structural and spectroscopic properties of the benzoisoxazole derivatives.

3. Results And Discussion

3.1. Structural Analysis

Firstly, the scan analysis was performed with B3LYP/6-311+G(d,p) level of theory. A potential energy surface (PES) scan was done by minimizing the potential energy in all geometrical parameters by changing the dihedral angle at every 30° (from 0° to 360°) with the rotation around the single bond (N1,C9—C10, X11; **X:** Cl, Br). The general representation of the dihedral angle (φ_1) determined from the scan analysis is given in Fig. 2.

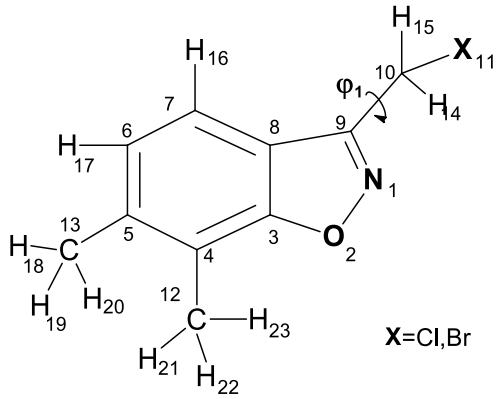

FIGURE 2. Numbering atoms for the definition of the bond lengths, bond angles, and dihedral angles.

From the scan analysis results, for each of the target molecules, we selected only one conformation which had the lowest energy value and hence the most stable conformer. The lowest energy conformers are shown in Fig. 3, along with the graph of change of total energy with dihedral angle. According to the conformational analysis results, the heteroatoms (oxygen and nitrogen) of the benzoisoxazole ring were on the different side to the halogen atoms in the 3- position of the benzoisoxazole. The conformational analysis results also show that the whole molecule is planar for both compounds and the minimum energies were obtained at 300º on the potential energy curve and the energy values for the compounds **1** and **2** are -3091.31 and -977.39 Hartree, respectively.

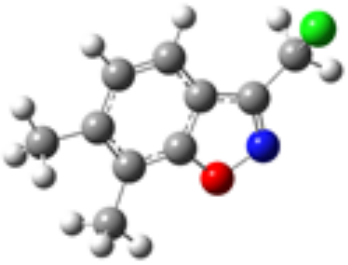

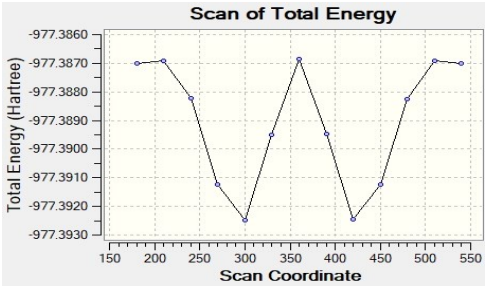

Energy: -3091.31 Hartree
Dihedral Angle: 0.86º

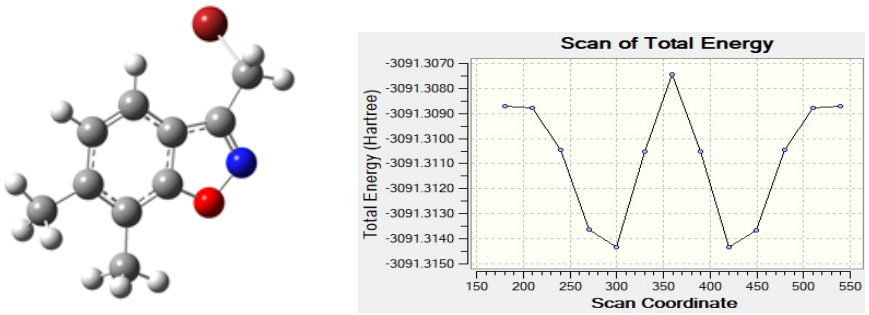

Energy: -977.39 Hartree
Dihedral Angle:-60,0º

FIGURE 3. Most stable conformers of the molecules and potential energy graph.

After determining the most stable conformers of the target compounds with the conformational analysis, we continued with the lowest conformers in next calculations and the geometry optimization of these conformers were performed by B3LYP/6-311+G(d,p) level of theory. The optimized structures of the studied compounds were given in Fig. 4. A search of the literature revealed that the molecule **1** was studied experimentally [11, 19], but that compound **2** was not present in any published computational or experimental studies. Experimental and calculated bond lengths of the studied compounds are given in Table 1.

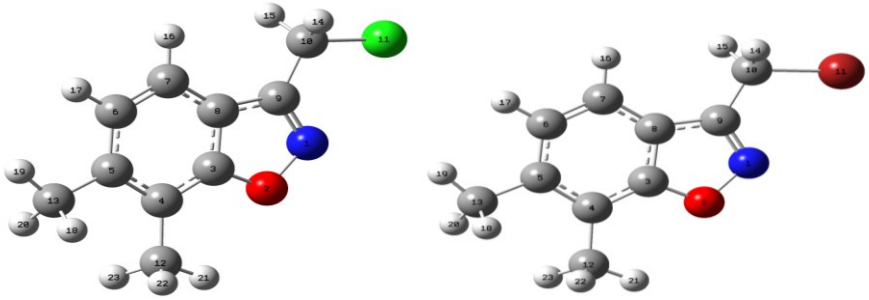

1 **2**

FIGURE 4. The optimized geometries of the target molecules.

As can be seen from the Table 1, after the geometry optimization, the calculated average bond lengths of the target molecules were 1.50 Å (C-C), 1.36 Å (C-O), 1.30 Å (C=N), 1.41 Å (O-N), 1.80 Å (C-Cl), 1.96 Å (C-Br) and between 1.39-1.44 Å (C = C). Due to the

conjugation in the aromatic heterocyclic benzoisoxale ring, all C=C bonds had an average C-C single and C=C double bond lengths values, as expected. Since only the experimental bond lengths of the molecule **1** were found in the literature, only the calculated values for molecule **1** were compared with the experimental values (X-Ray) [19]. The correlation coefficient (R^2) of experimental and calculated bond lengths for molecule **1** was found to be 0.861 (Fig. 5). Similarly, the correlation coefficient (R^2) between experimental and calculated bond angles for the title molecule **1** were 0.9658 (Fig. 5). Therefore, we can say that the calculated all bond lengths and bond angles of molecule **1** are in good agreement with the results obtained from X-ray analyses. We can conclude that the B3LYP/6-311+G(d,p) level of theory used in the calculation gives the correct results for these type molecules.

TABLE 1. Calculated bond lengths, bond angles and dihedral angles of the target compounds.

Bond Lengths (Å)				***Bond Angles (°)***			
Bond Type	**1 Expt***	**1 Calc.**	**2 Calc.**	**Bond Type**	**1 Expt***	**1 Calc.**	**2 Calc.**
N(1)-O(2)	1.417	1.407	1.407	N(1)-O(2)-C(3)	107.37	108.4	108.4
O(2)-C(3)	1.363	1.357	1.357	C(3)-C(4)-C(5)	114.78	115.3	115.3
C(3)-C(4)	1.387	1.396	1.396	C(4)-C(5)-C(6)	120.40	120.6	120.6
C(4)-C(5)	1.389	1.403	1.402	C(5)-C(6)-C(7)	123.19	122.5	122.5
C(5)-C(6)	1.406	1.414	1.414	C(6)-C(7)-C(8)	117.15	117.3	117.3
C(6)-C(7)	1.361	1.385	1.385	C(7)-C(8)-C(3)	118.97	119.5	119.5
C(7)-C(8)	1.397	1.399	1.399	C(8)-C(3)-C(4)	125.48	124.5	124.5
C(8)-C(9)	1.420	1.440	1.441	C(3)-C(8)-C(9)	103.89	103.2	103.2
C(8)-C(3)	1.372	1.395	1.395	C(8)-C(9)-N(1)	112.04	111.5	111.4
C(9)-C(10)	1.488	1.496	1.493	C(9)-N(1)-O(2)	106.82	107.2	107.2
C(9)-N(1)	1.295	1.301	1.301	C(9)-C(10)-X(11)	110.08	114.4	115.0
C(10)-X(11)	1.776	1.799	1.961	C(3)-C(4)-C(12)	121.25	121.3	121.3
C(4)-C(12)	1.498	1.506	1.506	C(5)-C(4)-C(12)	123.97	123.2	123.2
C(5)-C(13)	1.505	1.509	1.509	C(4)-C(5)-C(13)	120.5	119.9	119.9
C(6)-H(17)	0.930	1.084	1.084	C(6)-C(5)-C(13)	119.09	119.4	119.4
C(7)-H(16)	0.930	1.083	1.083	***Dihedral angles (°)***			
C(10)-H(14)	0.970	1.090	1.089	N(1)-O(2)-C(3)-C(4)	-178.95	180	179.99
C(10)-H(15)	0.970	1.090	1.089	O(2)-C(3)-C(4)-C(5)	177.83	-179.99	179.99
C(12)-H(21)	0.960	1.086	1.089	C(3)-C(4)-C(5)-(C6)	1,80	0.005	-0.001
C(12)-H(22)	0.960	1.094	1.094	C(4)-C(5)-(C6)-C(7)	-1.20	-0.002	0
C(12)-H(23)	0.960	1.094	1.094	C(5)-C(6)-C(7)-C(8)	-0.20	-0.003	0
C(13)-H(18)	0.960	1.094	1.094	C(6)-C(7)-C(8)-C(9)	-178.2	-179.9	179.99

C(13)-H(19)	0.960	1.090	1.090	N(1)-O(2)-C(3)-C(8)	0.20	0.0	-0.002
C(13)-H(20)	0.960	1.094	1.094	O(2)-C(3)-C(8)-C7)	-179.26	179.99	-179.99
-	-	-	-	C(8)-C(9)-C(10)-X(11)	58.8	179.9	179.9
-	-	-	-	N(1)-C(9)-C(10)-X(11)	-121.31	0.0	0.1

* Taken from reference 19

When we examine the rotation angles, it is observed that the results of the dihedral angles found by the geometry optimization of molecule **1** supported the results found by conformation analysis. However, there is a difference between experimental and calculated rotation angles of the molecule. Our calculation results show also that the benzoisoxazole ring and even the whole molecule are planar and the dihedral angle (φ_1) is almost 180°.

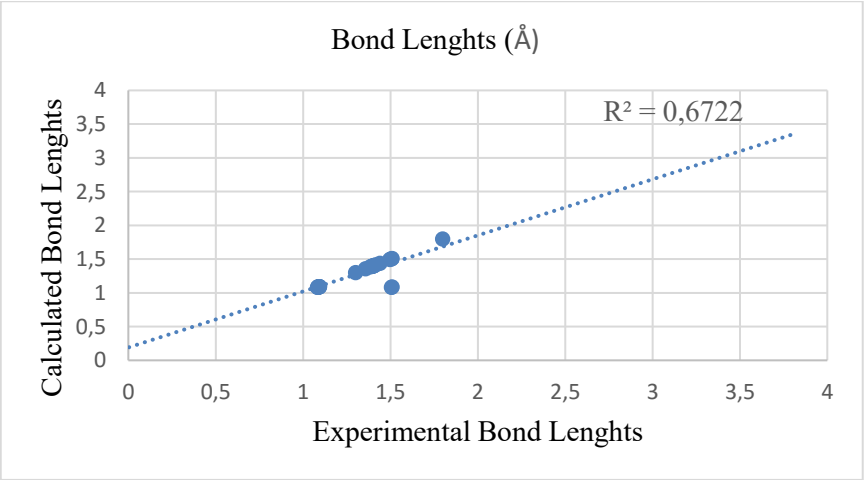

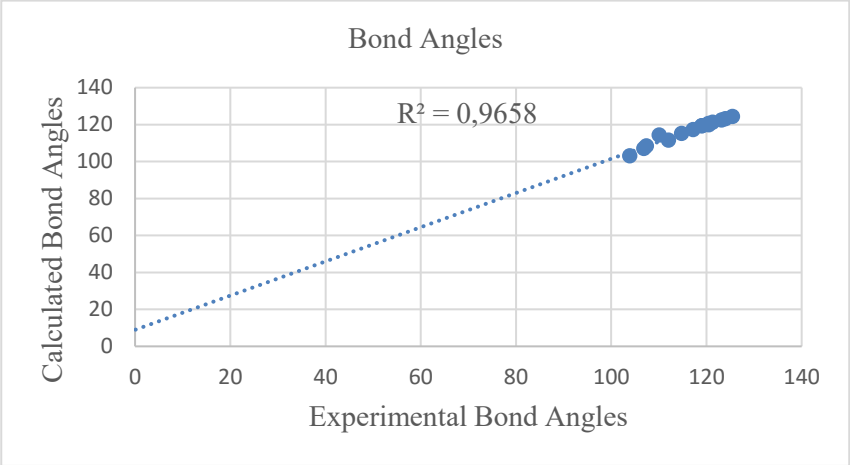

FIGURE 5. Bond lengths (upper) and bond angles (lower) correlation graphs for molecule **1**.

The X-Ray results of the molecule **1** show that the benzoisoxazole ring is planar and the torsion angle (φ_1) is 121.31° and the side chain is anticlinal looking down the C9—C10 bond [19]. The difference between computed and measured values can be explained that X-ray measurement is taken in a solid phase while calculation performed in the gas phase.

3.2. Energetics

The energies of the target molecules were based on the ground state and calculated with B3LYP/6-311+G(d,p) theory level in the gas phase and different solvents such as toluene, chloroform, THF, DCM, acetone, DMSO. The CPCM (conductor-like polarizable continuum) solvation method was used to compute condensed-phase energies in solvent systems. The total energies (E_T), the highest filled molecular orbital energies (E_{HOMO}) and the lowest empty molecular orbital (E_{LUMO}) energies, and the LUMO - HOMO energy difference (E_{gap}) were calculated. The zero point vibration energies (E_{ZPVEs}) were determined to convert the total electronic energy obtained from DFT calculations to 0 K total energy. The E_{ZPVEs} were corrected by a scaling factor of 0.967 for the B3LYP/6-311+G (d, p). Our energetic results are presented in Table 2. The results show that for both compounds, the zero point vibrational energies and the total energies in CPCM method are changed depending on the polarity of the solvent. In other words, both compounds have the lowest energy in DMSO, which has a higher dielectric constant. This can be explained by strong solvent-solute interactions in polar solvents. The calculation results revealed that all the energies, except the total energies (E_T), for both molecules are almost identical.

TABLE 2. Computed energies (E_{ZPVE}, $E_{T,}$ E_{HOMO}, $E_{LUMO,}$ and E_{gap}) of the studied molecules in the gas and different solvents.

Molecule 1	**Gas**	**Toluene**	**$CHCl_3$**	**THF**	**DCM**	**Acetone**	**DMSO**
$\mathbf{E_{ZPVE}}$ (kcal mol^{-1})	108.241	108.246	108.249	108.241	108.246	108.249	108.241
$\mathbf{E_T}$ (kcal mol^{-1})	-613211.460	-613215.001	-613216.536	-613217.151	-613217.336	-613217.866	-613218.101
$\mathbf{E_{HOMO}}$ (eV)	-6.821	-6.796	-6.785	-6.780	-6.779	-6.775	-6.774
$\mathbf{E_{LUMO}}$ (eV)	-1.543	-1.545	-1.550	-1.552	-1.553	-1.556	-1.557
$\mathbf{E_{gap}}$ (eV)	5.279	5.251	5.235	5.228	5.226	5.219	5.216
Molecule 2							
$\mathbf{E_{ZPVE}}$ (kcal mol^{-1})	107.728	107.764	107.778	107.782	107.784	107.788	107.787
$\mathbf{E_T}$ (kcal mol^{-1})	-1939717.861	-1939721.355	-1939722.864	-1939723.469	-1939719.973	-1939724.170	-1939724.405
$\mathbf{E_{HOMO}}$ (eV)	-6.820	-6.795	-6.784	-6.779	-6.778	-6.774	-6.772
$\mathbf{E_{LUMO}}$ (eV)	-1.542	-1.545	-1.549	-1.551	-1.552	-1.554	-1.556
$\mathbf{E_{gap}}$ (eV)	5.278	5.250	5.234	5.228	5.226	5.219	5.216

The HOMO and LUMO are named as frontier molecular orbitals (FMOs). The FMOs play an important role in the optical and electrical properties, as well as in UV–VIS spectra [20]. The energy difference (E_{gap}) characterizes the chemical reactivity and kinetic stability of molecules. A molecule with a small E_{gap} is usually associated with a high chemical reactivity and also termed as soft molecule [20]. As mentioned above, the HOMO and LUMO energies and their energy difference (E_{gap}) of the target molecules were computed and their HOMO and LUMO graphs in the gas phase were generated from the optimized geometry using GaussView 05 program and are depicted in Fig. 6. The HOMO and LUMO graphics show π molecular orbital characteristics and the electronic cloud distribution of both molecular orbitals are mainly localized on the benzoisoxazole ring system as seen from Fig. 6. The calculation results show that the band gaps are very similar for both optimized molecules. In the case of solvent systems, in going from low-polarity solvent to high-polarity solvent, the HOMO energy increases while the LUMO energy decreases. As a natural consequence of this, the E_{gap} values decrease in the same polarity order for both compounds.

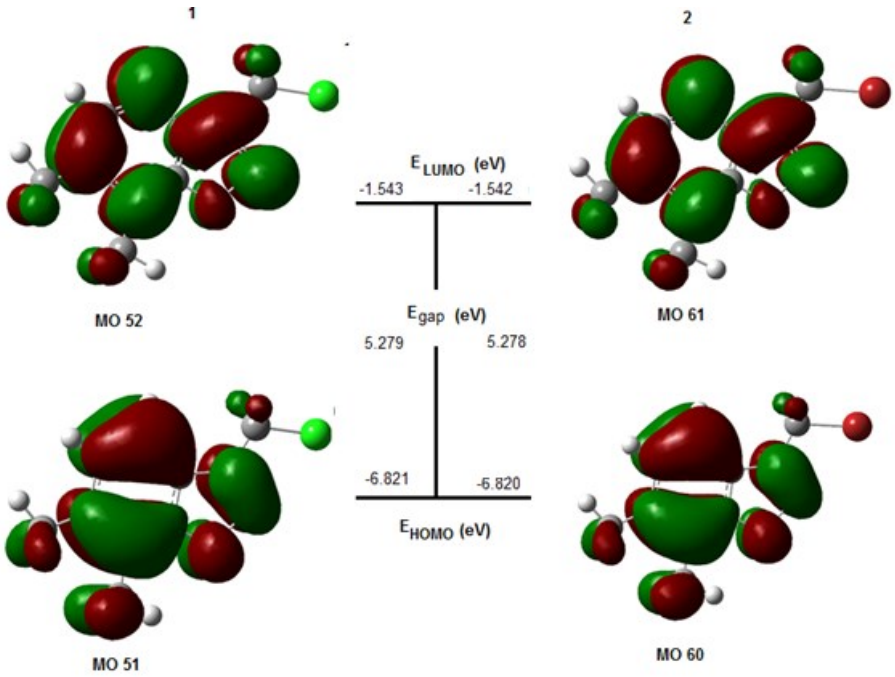

FIGURE 6. HOMO and LUMO graphs of the title compounds in the gas phase

3.3. Spectroscopic Analysis

In this part, UV, IR, ^{1}H-NMR and ^{1}3C-NMR spectra calculated by B3YLP/6-311+ G (d,p) theory level for the target molecules **1** and **2** are described.

UV Analysis

The maximum absorption wavelengths (λ_{max}) in the ultraviolet spectra of the title compounds in the gas phase and different solvents were calculated using the TD-DFT with B3LYP functional and 6-311+G(d,p) basis set. To observe solvent effects Conductor-like Polarizable Continuity Model (CPCM) [21] was used in TD-DFT calculations and dichloromethane, chloroform, tetrahydrofuran, acetone, ethanol, and dimethyl sulfoxide were chosen as solvents. The computed λ_{max1} and λ_{max2} values of the title compounds in the gas phase and the solvent systems are presented in Table 3 and their electronic absorption spectra are given in Fig. 7. There is not experimental UV spectral data of the title compounds, the benzoisoxazole without substituent and 6,7-dimethylbenzoisoxazole in the literature, therefore we could not compare our calculation results to the experimental values and we

evaluated our UV calculation results for gas phase and different solvent systems. From the results, it is revealed that the absorption maxima of the compounds exhibited two distinct absorption bands, attributed to $\pi \rightarrow \pi^*$ transitions. The calculated characteristic peaks (λ_{max1}) of benzoisoxazoles in the gas phase are sharp and observed at 203.5 and 249.5 nm for the molecules **1** and **2**, respectively**.** In gas-phase calculations, the moderate absorbance peak (λ_{max2}) for molecule **1** was found at 252.0 nm, while the same peak was not found for molecule **2**. Since the Cl atom is more electronegative than Br, the λ_{max1} wavelength of molecule **1** were obtained at a lower wavelength than that of molecule **2** in the gas phase.

TABLE 3. Calculated wavelengths λ_{max1} and λ_{max2} (in nm) for title molecules.

Phase/Solvent	**1**		**2**	
	λ_{max1}	**λ_{max2}**	**λ_{max1}**	**λ_{max2}**
Gas	203.5	252.0	249.5	-
Chloroform	188.0	228.0	189.5	227.5
Tetrahydrofuran	206.5	250.0	189.0	227.5
Dichloromethane	188.0	227.5	189.0	227.5
Acetone	189.5	227.5	189.0	227.5
Dimethyl sulfoxide	190.0	227.5	189.5	228.0
Ethanol	189.5	227.5	188.5	227.5

In all solvent systems, two characteristic peaks for both compounds were obtained one sharp and the other broad, as in the gas phase. In all solvent systems except THF, the absorption bands at almost the same wavelengths for both compounds were also obtained. Namely, the λ_{max1} wavelengths in all solvent systems, except THF, for both compounds, were found in the range of 188-190 nm, while the broad absorption bands (λ_{max2}) were determined as 228 nm. The λ_{max1} and λ_{max2} for molecule **1** in THF are 206.5 and 250.0 nm, respectively. Molecule **1** in THF shows a bathochromic shift (~17-22 nm) resulting in absorption in the UV region. In all other solvent systems, the λ_{max1} and λ_{max2} absorption bands shifted to the lower wavelengths than the wavelengths found in the gas phase. In the case of both compounds, the λ_{max1} and λ_{max2} wavelengths varied little with solvent type, except THF for molecule **1**.

Analysis of the wave functions indicates that the electron absorption (λ_{max1}) corresponds to the transition from the ground to the first excited state and is generally described by the one-electron transition from HOMO energy level to LUMO energy level. The calculation results

showed that $E_{HOMO} \rightarrow E_{LUMO}$ transition, which is the most fundamental transitions, were 51→52 for molecule **1** and 60→61 for molecule **2** (see Fig. 6).

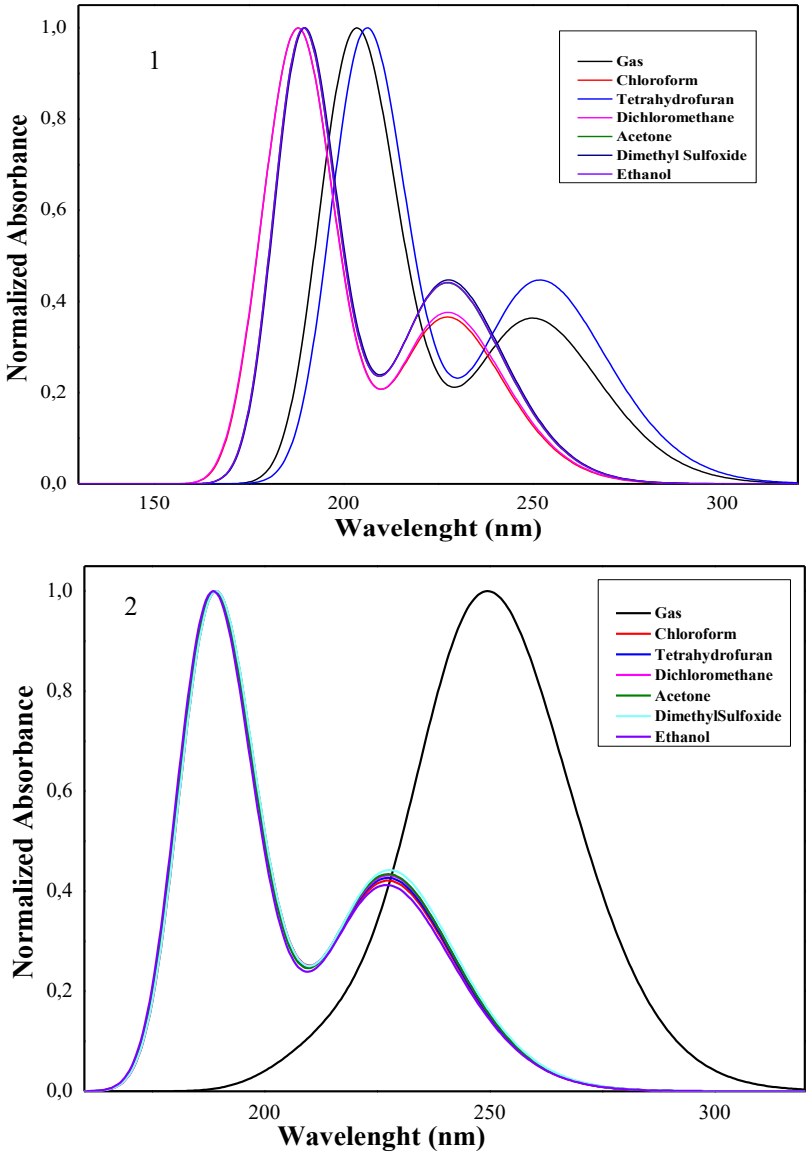

FIGURE 7. Calculated UV spectra for molecules **1** and **2** in gas and various solvents.

IR Analysis

In this section, the calculated vibrations of the target compounds are discussed and the calculation results for molecule **1** are compared with its experimental values. All frequency values calculated with B3YLP/6-311+G(d,p) method were obtained with the harmonic approximation in the gas phase. The calculated IR spectra of the title molecules are given in Fig. 8.

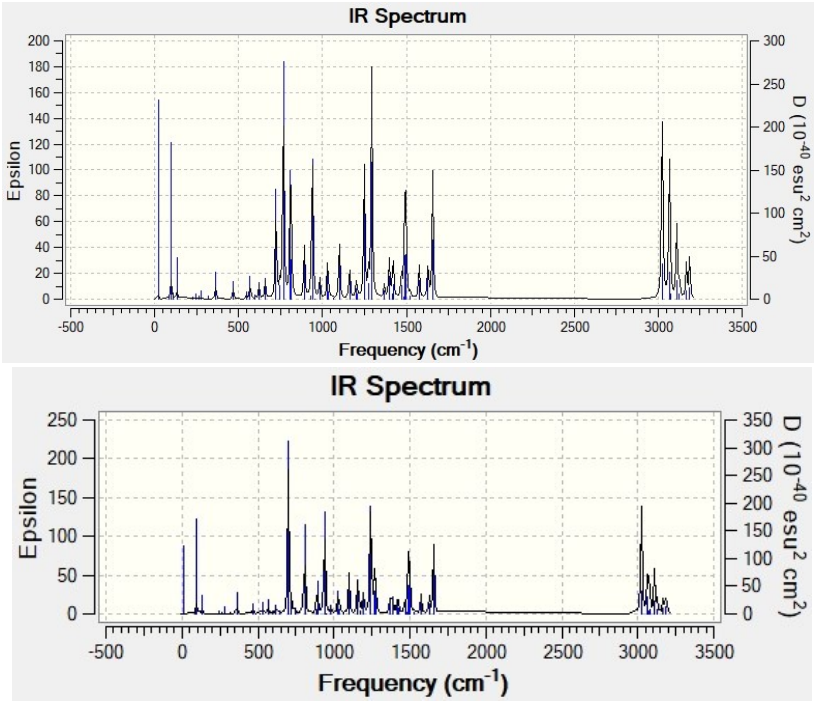

FIGURE 8. Calculated IR spectra of the title compounds.

The vibrational wavenumbers obtained by DFT calculations are generally overestimated than the experimental values due to the neglect of anharmonicity in the real system. These discrepancies can be corrected either by computing with anharmonic approximation or by multiplying with a scaling factor. To compensate these systematic errors the calculated vibrational frequencies for the target compounds in the gas phase are corrected by using a scaling factor (0.9688) [22] for B3LYP/6-311+G(d,p) level of theory. Both molecules have 23 atoms and hence there are 63 normal modes of vibrations. Instead of discussing all

individual modes, the most characteristic peaks are selected and unscaled and scaled vibrational frequencies for the molecules **1** and **2** are presented in Table 4.

TABLE 4. Selected IR absorption bands (cm^{-1}) for molecules **1** and **2**.

	1			**2**		
N	**Expt.***	**Unscaled**	**Scaled**	**Unscaled**	**Scaled**	**Assignments**
1	3019	3167.9	3069.1	3168.1	3069.3	Aromatic C-H
2	2970	3070.0	2974.2	3081.8	2985.6	Aliphatic X-C-H
3	2923	3022.4	2928.1	3022.5	2928.2	Aliphatic C-H
4	1604	1656.9	1605.2	1656.3	1604.6	Aromatic C=C
5	-	1575.4	1526.2	1574.0	1524.9	Aromatic C=N
6	1390	1423.5	1379.1	1423.4	1379.0	C-C stretching
7	-	1273.6	1233.9	1274.2	1234.4	C-O stretching
8		940.0	910.7	938.9	909.6	N-O stretching
9	697	767.1	743.2	-	-	C-Cl stretching
10	-	-	-	699.4	677.6	C-Br stretching

***** Taken from reference 19

The heteroaromatic rings have highly extremely characteristic peaks such as aromatic C-H and aromatic C=C stretching vibrations. Aromatic C-H stretching vibrations are normally observed in the range of 3100-3000 cm^{-1} [23]. The experimental value for molecule **1** is 3019 cm^{-1} while our calculated value of this mode is 3069.1 cm^{-1}. There is a little difference between experimental and calculated vibrational frequencies because experimental results are taken in solvent phase while theoretical results are obtained in the gas phase. It is thought that another reason for this difference is the harmonic approach used for calculations while many modes have anharmonic character, experimentally. Aromatic C = C stretching vibrations are generally observed between 1600-1400 cm^{-1}. The experimental aromatic C = C vibration for molecule **1** was 1604 cm^{-1} and the corresponding calculated value is 1605.2 cm^{-1}. The calculated remaining bands of the benzoisoxazole ring at 1526.2, 1233.9 and 910.7 cm^{-1} are assigned for C = N, C-O, and N-O ring stretching vibrations, respectively.

Aliphatic C-H vibrational frequencies of the methyl and methylene groups connected aromatic rings are normally expected in the range of 3100-2900 cm^{-1} and the experimental aliphatic C-H stretching vibration of the molecule **1** is observed at 2923 cm^{-1} and the

vibrational wavenumber computed at 2928.1 cm^{-1} is assigned to aliphatic C-H stretching. Similarly, aliphatic X-C-H stretching vibration of molecule **1** is experimentally observed at 2970 cm^{-1} and the band calculated at 2974.2 cm^{-1} is assigned as X-C-H stretching. Finally, experimental C-Cl stretching vibration is observed at 697 cm^{-1} and the calculated corresponding value is 743.2 cm^{-1}. The result computed by B3LYP/6-31+G(d,p) presents that the vibrational wavenumber at 677.6 cm^{-1} is assigned to the C-Br stretching vibration for molecule **2**. Also, according to the computed results, the vibrational frequencies of molecules **1** and **2** are very similar and the difference in the electronegativity of the substituents had little effect on other vibrations. To make a comparison with the experimental and computed IR frequencies for molecule **1**, we made a correlation graph shown in Fig. 9. As can be seen in Fig. 9, there is a good correlation between the experimental and the calculated scaled fundamental vibrational of molecule **1** (R^2=0.9993).

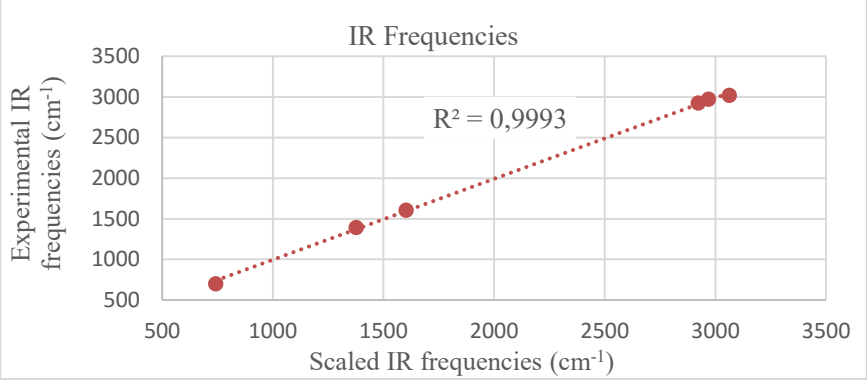

FIGURE 9. IR correlation graph for molecule **1**

NMR Analysis

The ^{1}H and ^{13}C-NMR chemical shifts of the title molecules optimized by B3YLP/6-311+G (d,p) were calculated at the same level of theory by the GIAO (Gauge-Independent Atomic Orbital) [24, 25] approach and referenced by TMS. First, the shielding of tetramethylsilane (TMS), which is used as a general standard, was computed using the B3YLP/6-311+G(d,p) level of theory. Then, the chemical shifts of the title compounds were calculated with the theory used in the geometry optimization of the molecules. The subtracting of two evaluated values ($\sigma_{TMS} - \sigma_{comp.}$) gives the desired chemical shifts of the molecules. The calculated ^{1}H and ^{13}C isotropic chemical shielding of TMS at the B3LYP/6-311+G(d,p) level in the gas phase are 31.98 and 183.96 ppm, respectively. The numbering of atoms in the molecules for

^{1}H-NMR and ^{13}C-NMR is presented in Fig. 10. The ^{1}H-NMR spectra of both compounds were calculated in a $CDCl_3$ solvent are presented in Fig. 11. The calculated values of ^{1}H and ^{13}C chemical shifts in the gas phase together with experimental values, only available in the literature for compound **1**, are presented in Table 5.

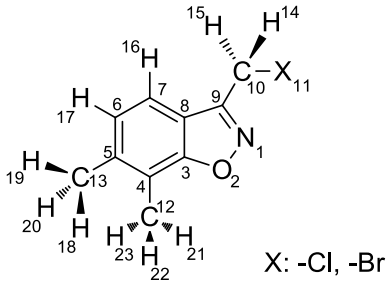

FIGURE 10. Numbering atoms for ^{1}H-NMR and ^{13}C-NMR.

Both molecules have three types of protons, which are aromatic, methyl and methylene. In calculated ^{1}H-NMR spectra, the aromatic protons (H16 and H17) of benzoisoxazole ring appeared in the range of 7.2-7.6 ppm and the corresponding experimental values are at 7.17 and 7.52 ppm for the molecule **1**. For both molecules, the calculated methyl protons (H18-H23) bound to the benzoisoxazole ring at positions 6 and 7 were found in the range 2.1- 3.4 ppm and experimentally observed methyl protons were at 2.43 and 2.47 ppm for molecule **1**. The signals calculated at 5.2 ppm for molecule **1** and 4.6 ppm for molecule **2** were assigned as methylene protons (H14 and H15) of both compounds and the corresponding methylene protons were experimentally observed at 4.88 ppm for molecule **1**. There is a good correlation between experimental and calculated proton signals of molecule **1** and the maximum deviation is 0.53 ppm, except H23 proton of the methyl group. However, the deviation of the experimental and calculated value of H23 proton was 0.93 ppm. This may be due to the weak H bond between the oxygen (O2) and methyl hydrogen (H23) of the benzoisoxazole ring. According to the calculation results, the length of this H bond is 2.53 Å.

1

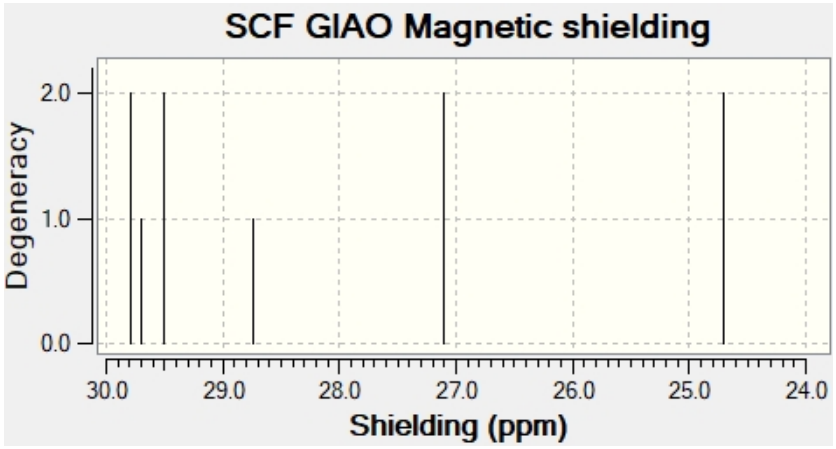

2

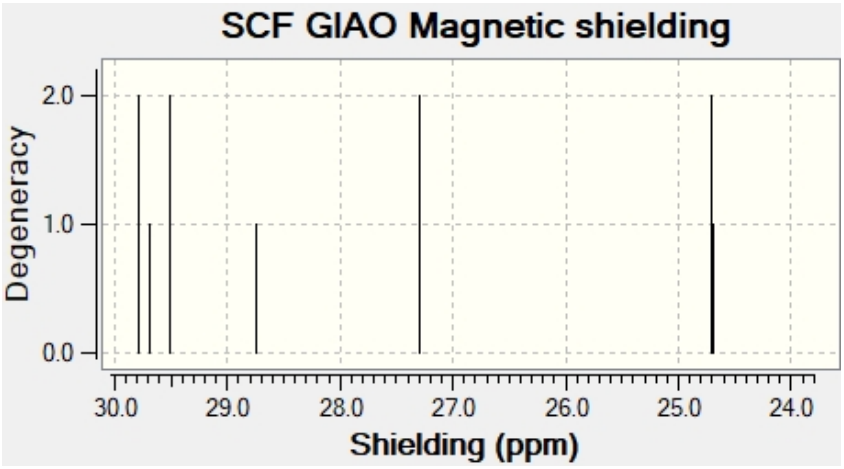

FIGURE 11. Calculated ^{1}H-NMR spectra of the title compounds.

TABLE 5. Experimental and calculated ^{1}H-NMR and ^{13}C-NMR isotropic chemical shifts (ppm) for title molecules.

Atom	**1**		**2**
	Cal.	**Expt.***	**Cal.**
H-14	5.2	4.88	4.6
H-15	5.2	4.88	4.6
H-16	7.6	7.52	7.2
H-17	7.5	7.17	7.2
H-18	2.5	2.43	2.4
H-19	2.4	2.43	2.2
H-20	2.5	2.43	2.4
H-21	3.0	2.47	3.2
H-22	2.3	2.47	2.1
H-23	3.4	2.47	2.1
C-3	171.5	163.5	171.8
C-4	126.8	118.7	126.8
C-5	146.8	139.0	146.8
C-6	131.2	126.5	131.3
C-7	120.9	117.5	121.1
C-8	124.1	117.7	124.6
C-9	160.6	155.1	160.7
C-10	47.3	35.1	39.8
C-12	13.3	11.7	13.3
C-13	22.1	19.1	22.1

*Taken from reference 19

The ^{13}C NMR spectra of both compounds were calculated in a $CDCl_3$ solvent and are presented in Fig. 12. In the ^{13}C NMR spectra of the compounds, calculated signals at δ 120.9, 124.1, 126.8, 131.2, 146.8, 160.6, and 171.5 ppm are corresponding to carbon atoms (C3-C9) of the benzoisoxazole ring. The corresponding experimental values for molecule **1** are 117.5, 117.7, 118.7, 126.5, 155.1, and 163.5 ppm in the literature [19]. The values of the methyl carbons (C12 and C13) linked to benzoisoxazole ring were calculated as 13.3 and 22.1 ppm for both molecules and experimental values of these carbon peaks are observed at

11.7 and 19.1 ppm [19]. The signal for methylene carbon (C10) linked to chlorine atom is experimentally observed at 35.1 ppm and theoretically at 47.3 ppm for molecule **1**. The peak of the same carbon in molecule **2** was calculated as 39.8 ppm because this carbon in molecule **2** is bound to the bromine, whose electronegativity less than chlorine. Hence, it gives a signal in an upfield. The maximum deviation between the calculated and experimental carbon signals of molecule **1** is 8.1 ppm, except C10 carbon of the methylene. However, the maximum deviation in ^{13}C-NMR is higher than ^{1}H NMR chemical shifts.

1

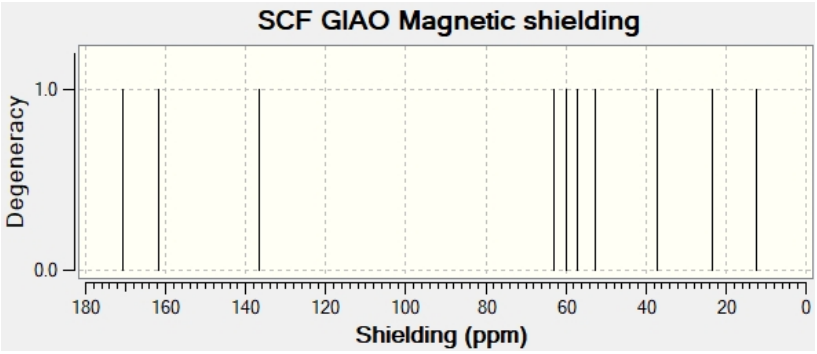

2

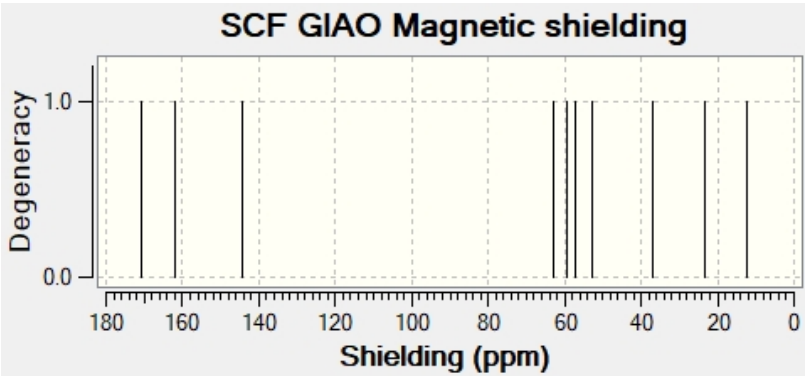

FIGURE 12. Calculated ^{13}C-NMR spectra of the title compounds.

The correlation graphs obtained from the comparison of the experimental and calculated results of ^{1}H-NMR and ^{13}C-NMR for molecule **1** are depicted in Fig. 13. The results show that the calculated chemical shifts are in line with the experimental values of compound **1**. The correlation coefficients (R^2) found for molecule **1** are 0.9769 and 0.9972 for ^{1}H and ^{13}C-NMR, respectively. However, small differences may be because the calculations were done

in the gas phase, while the experimental values measured in the $CDCl_3$ solution, where the molecular interactions are important. Even so, it can be concluded that the GIAO method and B3LYP/6-311+G(d,p) level of theory is sufficient to calculate ^{1}H and ^{13}C-NMR chemical shifts of the studied compounds.

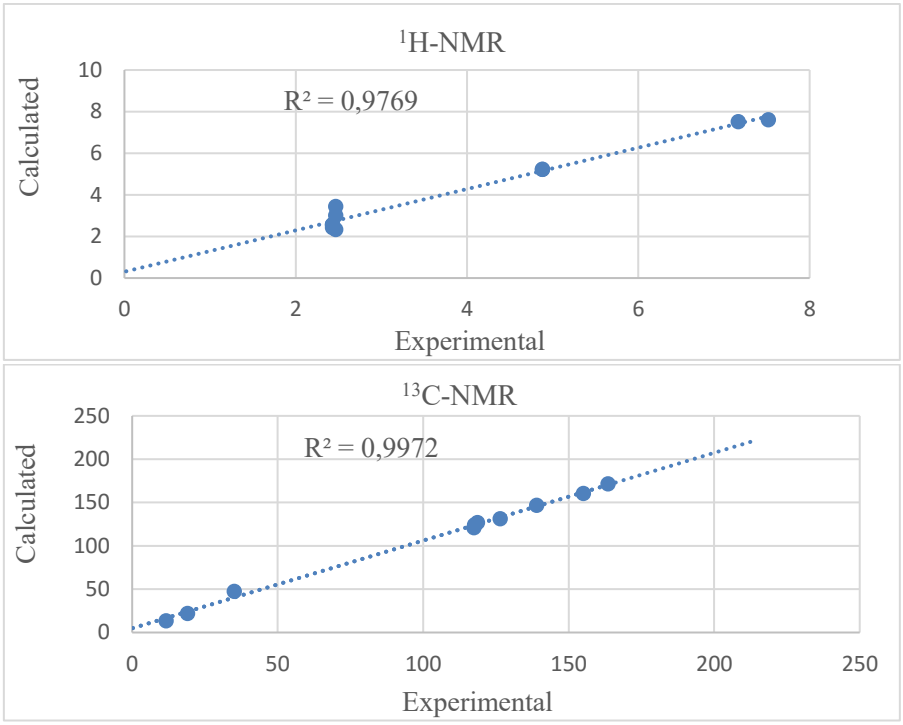

FIGURE 13. Comparison of the experimental and calculated ^{1}H (upper) and ^{13}C-NMR (lower) values of the compound **1**.

4. Conclusion

In this work, firstly the molecular structural parameters such as bond length, bond angle, and dihedral angle for two benzoisoxale derivatives were calculated and compared to the experimental values of molecule **1**. Calculations done by DFT method were carried out with the gas phase and in various solvent systems. The calculated geometric parameters by using density functional theory (DFT) with the 6-311+G(d,p) basis set are in good agreement with the X-ray structure of the molecule **1**. Then, the energies and spectroscopic properties of the molecules were computed. The B3LYP/6-311+G(d,p) level of theory was used to determine

the most stable conformations, energetics, the structural and spectral properties. The total energies, the highest filled molecular orbital energies, the lowest empty molecular orbital energies, and the LUMO - HOMO energy difference were calculated. It is found that the zero-point vibrational energies and the total energies in CPCM method varied depending on the polarity of the solvent. The calculated HOMO, LUMO energies and band gaps of both molecules are very similar for both compounds. Then, the maximum absorption wavelengths (λ_{max}) in the ultraviolet spectra of the title compounds in the gas phase and different solvents were calculated using the TD-DFT with B3LYP/6-311+G(d,p). Two characteristic peaks for both compounds were obtained one sharp and the other broad. In all solvent systems except THF, the absorption bands at almost the same wavelengths for both compounds were also obtained. The vibrational band assignments were performed at B3LYP/6-311++G(d,p) theory level to compare the experimental (FT-IR) and calculated vibrational frequencies of the compound **1**. A good correlation between the observed and scaled IR frequencies was obtained for compound **1**. Scaled results seem to be in good agreement with the experimental ones. Finally, the ^{1}H and ^{13}C-NMR chemical shifts of the title molecules were calculated at the same level of theory by the GIAO approach. The results show that the calculated chemical shifts are in good agreement with the experimental values of compound **1**. Because of the compatibility of the calculated and experimental results of molecule **1**, the B3LYP level with 6-311+G(d,p) basis set can be considered as a suitable method for similar molecules to understanding the energetics, structural and spectral properties.

ÖZET

Bu çalışmada, iki benzisoksazol türevinin özelliklerini belirlemek için teorik hesaplamalar yapılmıştır. Kuantum kimyasal hesaplamalarda, 6-311+G(d,p) temel seti ile Yoğunluk Fonksiyonel Teorisi (DFT) kullanılmıştır. Hesaplamalar, gaz fazında ve toluen, kloroform, THF, DCM, aseton, DMSO gibi farklı çözücü sistemlerinde gerçekleştirilmiştir. Çözücü sistemlerde enerjileri hesaplamak için CPCM (conductor-like polarizable continuum) solvasyon modeli kullanılmıştır. Hedef moleküllerin yapısal parametreler (bağ uzunlukları, bağ açıları ve dönme açılar), enerjileri (toplam enerjiler, sıfır noktası titreşim enerjileri, sınır orbital enerjileri (E_{HOMO}, E_{LUMO} ve bant aralığı enerjileri) ve spektroskopik özellikleri (UV, IR, ^{1}H-NMR ve ^{13}C-NMR) belirlenmiştir. Molekül 1 için deneysel değerler literatürde bulunduğu için hesaplama sonuçları literatür değerleri ile karşılaştırılmıştır. Molekül 1 için hesaplanan geometriler deneysel verilerle hata sınırları içinde uyuşmaktadır. IR frekansları durumunda ise, ölçeklendirilmiş hesaplanan frekansların deneysel sonuçlarla uyuştuğu anlaşılmıştır. Ayrıca, molekül 1'in deneysel ve hesaplanmış proton sinyalleri (R^2 = 0.9769) ve karbon sinyalleri (R^2 = 0.9972) arasında iyi bir ilişki bulunmuştur.

References

[1] K. Ha, H. S. Lim and H. J. Kim, 5-(4-Chlorophenyl)-6-isopropyl-5,6-dihydro-4H-pyrrolo[3,4-c]isoxazole. Acta Crystallographica, E66 (2010) o2483.

[2] K. V. N. Raju, M. Krishnaiah, N. J. Kumar and S. N. Rao, Structure conformation of 4-(4-methoxyphenyl)-5-phenyl isoxazole. Acta Crystallographica, A58 (2002) c128.

[3] M. Krishnaiah, R. R. Kumar, T. Oo and P. Kaung, 4-(4-Chlorophenyl)-5-phenylisoxazole. Acta Crystallographica, E65 (2009) o2324.

[4] H. Hasegawa, Utilization of zonisamide inpatients with chronic pain orepilepsy refractory to other treatments: a retrospective, open label, uncontrolled study in a VA hospital. Current Medical Research and Opinion, 20/5 (2004) 577-580.

[5] Y. Masuda, Y. Utsui, Y. Sharashi, T. Karasawa, K. Yoshida and M. Shimizu, Relationships between plasma concentrations of diphenylhydantoin, phenobarbital, carbamazepine, and 3-sulfamoylmethyl-1,2-benzoisoxazole (AD-810), a new anticonvulsant agent, and their anticonvulsant or neurotoxic effects in experimental animals. Epilepsia, 20/6 (1979) 623-633.

[6] H. Uno, M. Kurukova, Y. Masuda and H. Nishimura, Studies on 3-substituted 1,2-benzoisoxazole derivatives. 6. Syntheses of 3-(sulfamoylmethyl)-1,2-benzoisoxazole derivatives and their anticonvulsant activities. Journal of Medicinal Chemistry, 22/2 (1979) 180-183.

[7] G. V. Bossche, Y. G. Gelders and S. L. Heylen, Development of new antipsychotic drugs. Acta psiquiátrica y psicológica de América Latina, 36 (1990) 13-25.

[8] M. Shimizu, T. Karasawa, M. Masuda and M. Oka, 1,2-Benzoisoxazole-3-acetamidoxime hydrochloride, a new psychotropic agent. Experientia, 30/4 (1974) 405-405.

[9] M. Jain and C. H. Kwon, 1,2-Benzoisoxazole Phosphorodiamidates as Novel Anticancer Prodrugs Requiring Bioreductive Activation. Journal of Medicinal Chemistry, 46/25 (2003) 5428-5436.

[10] K. A. Thakar and B. M. Bhawal, Synthesis and Antimicrobial screening of amino-1, 2-Benzoisoxazoles and sulphanilamido-1, 2 benzoisoxazoles. Current Science, 47/24 (1978) 950-952.

[11] V. R. Arava, G. Laxminarasimhulu, U. B. R. Siripalli and P. K. Dubey, An efficient synthesis of 3-chloromethyl-1,2-benzoisoxazoles via modified Boekelheide rearrangement. Indian Journal of Chemistry, 50B/1 (2011) 119-125.

[12] W. Kohn and L.J. Sham, Self-Consistent Equations Including Exchange and Correlation Effects. Physical Review, 140A (1965) 1133–1138.

[13] M. J. Frisch, G. W. Trucks, H. B. Schlegel, G. E. Scuseria, M. A. Robb, J. R. Cheeseman, G. Scalmani, V. Barone, B. Mennucci, G. A. Petersson, H. Nakatsuji, M. Caricato M, X. Li, H. P. Hratchian, A. F. Izmaylov, J. Bloino, G. Zheng, J. L. Sonnenberg, M. Hada, M. Ehara, K. Toyota, R. Fukuda, J. Hasegawa, M. Ishida, T. Nakajima, Y. Honda, O. Kitao, H. Nakai, T. Vreven, J. A. Montgomery, J. E. Peralta, F. Ogliaro, M. Bearpark, J. J. Heyd, E. Brothers, K. N. Kudin, V. N. Staroverov, R. Kobayashi, J. Normand, K. Raghavachari, A. Rendell, J.C. Burant, S. S. Iyengar, J. Tomasi, M. Cossi, N. Rega, J. M. Millam, M. Klene, J. E. Knox, J. B. Cross, V. Bakken, C. Adamo, J. Jaramillo, R. Gomperts, R. E. Stratmann, O. Yazyev, A. J. Austin, R. Cammi, C. Pomelli, J. W. Ochterski, R. L. Martin, K. Morokuma, V. G. Zakrzewski, G. A. Voth, P. Salvador, J. J. Dannenberg, S. Dapprich, A. D. Daniels, Ö. Farkas, J. B. Foresman, J. V. Ortiz, J. Cioslowski and D. J. Fox (2009) Gaussian 09, Revision D.01. Gaussian, Inc., Wallingford CT.

[14] R. Dennington, T. Keith, and J. Millam, (2009) GaussView, Version 5.0.8.

[15] A. D. Becke, Density-functional exchange-energy approximation with correct asymptotic behavior. Physical Review A, 38 (1988) 3098–3100.

[16] C. Lee, W. Yang and R. G. Parr, Development of the Colle-Salvetti correlation-energy formula into a functional of the electron density. Physical Review B, 37 (1988) 785–789.

[17] K. Raghavachari, J. S. Binkley, R. Seeger and J. A. Pople, Self consistent molecular orbital methods. XX. A basis set for correlated wave functions. Journal of Chemical Physics, 72 (1980) 650-654.

[18] P. Ü. Civcir**,** G. Kurtay and K. Sarıkavak, Experimental and theoretical investigation of new furan and thiophene derivatives containing oxazole, isoxazole, or isothiazole subunits. Structural Chemistry, 28/3 (2017) 773–790.

[19] M. Kayalvizhi, G. Vasuki, A. Veerareddy and G. Laxminarasimha, 3-Chloromethyl-6,7-dimethyl-1,2-benzoxazole. Acta Crystallographica Section E, 68/10 (2012) o3008-o3008.

[20] I. Fleming, Frontier Orbitals and Organic Chemical Reactions. Wiley, London, 1976.

[21] R. E. Stratmann, G. E. Scuseria and M. J. Frisch, An efficient implementation of time-dependent density-functional theory for the calculation of excitation energies of large molecules. Journal of Chemical Physics, 109/19 (1998) 8218-8224.

[22] J. P. Merrick, D. Moran and L. Radom, An Evaluation of Harmonic Vibrational Frequency Scale Factors. Journal of Physical Chemistry A, 111/45 (2007) 11683–11700.

[23] E. Erdik, Organik Kimyada Spektroskopik Yöntemler. Gazi Kitabevi, Ankara, 2015.

[24] K. Wolinski, J. F. Hinton and P. Pulay, Efficient implementation of the gauge-independent atomic orbital method for NMR chemical shift calculations. Journal of the American Chemical Society, 112/23 (1990) 8251–8260.
[25] R. Ditchfield, Self-consistent perturbation theory of diamagnetism. Molecular Physics, 27/4 (1974) 789–807.

Current Address: EZGİ ÖZEN: Department of Chemistry, Ankara University, 06100 Ankara, TURKEY
E-mail Address: ozenezgi@ankara.edu.tr
ORCID: http://orcid.org/0000-0002-4433-813X

Current Address: MELİKE KALKAN: Department of Chemistry, Ankara University, 06100 Ankara, TURKEY
E-mail Address: mkalkan@ankara.edu.tr
ORCID: http://orcid.org/0000-0001-5461-7151

Current Address: PERVİN ÜNAL CİVCİR (Corresponding author): Department of Chemistry, Ankara University, 06100 Ankara, TURKEY
E-mail Address: civcir@science.ankara.edu.tr
ORCID: https://orcid.org/0000-0003-0331-4091